2005 International Symposium on Nonlinear
Theory and its Applications (NOLTA2005)
Bruges, Belgium, October 18-21, 2005

Some significant bifurcation curves in a hysteresis oscillator

Federico Bizzarri†, Daniele Stellardo†, Marco Storace†, Oscar De Feo‡

†Biophysical and Electronic Engineering Department, University of Genoa
Via Opera Pia 11a, I-16145 Genova, Italy
‡Laboratory of Nonlinear Systems, Swiss Federal Institute of Technology Lausanne (EPFL)
EPFL-I&C-LANOS, CH-1015 Lausanne, Switzerland
Email: Marco.Storace@unige.it

Abstract—In this paper we propose a bifurcation analysis of a set of ordinary differential equations describing a circuit oscillator based on hysteresis. We resort to continuation methods and to the theory of normal forms to find out some significant bifurcation curves.

1. Introduction

The hysteretic oscillator this paper deals with has been extensively studied in the last few years, by modelling the nonlinear part of the circuit in two different ways [1, 2, 3, 4, 5, 6]. Up to now, the oscillator bifurcation scenario has been studied mainly through brute-force analyses (excepted for [5]), which are strongly dependent on the initial conditions and do not allow to easily find either unstable invariant sets or coexisting invariant sets (even if stable). In this paper, the bifurcation analysis of the circuit will be carried out by combining numerical continuation techniques (by resorting to tools such as AUTO2000 [7]) and normal forms theory [8]. The normalized system of equations modelling the dynamics of the hysteresis oscillator can be written as follows:

$$\begin{cases} \dot{x}_1 = -(x_1 + x_2) & (1a) \\ \dot{x}_2 = (2 + p_1)(x_1 + x_2) - x_2 - p_2 x_3 & (1b) \\ \dot{x}_3 = p_3(\Psi - p_4 \sinh(x_3)) & (1c) \\ x_1 - x_3 = \operatorname{asinh}\left(\frac{\Psi}{p_5}\right) + \Psi & (1d) \end{cases} \tag{1}$$

The first three equations can be written, more compactly, as $\dot{\boldsymbol{x}} = \boldsymbol{f}(\boldsymbol{x}; \boldsymbol{p})$, where $\boldsymbol{x} = (x_1, x_2, x_3)$ is the state vector, $\boldsymbol{p} = (p_1, p_2)$ is the bifurcation parameter vector, whereas $p_3 = 300$, $p_4 = 2.97E-24$, and $p_5 = 77.22E-12$ are fixed. Equations (1a) and (1b) are both linear. The only nonlinear equation of the ODE system (1a)–(1c) is Eq. (1c), where the function Ψ is implicitly defined in Eq. (1d).

2. Some general properties

Generally speaking, the two (linear and nonlinear) parts of the circuit are bidirectionally coupled through the parameters p_2 (coupling from the nonlinear part to the linear part) and p_3, p_4, p_5 (*viceversa*). We point out that, for $p_2 = 0$, the coupling becomes one-directional, thus determining degeneracies, as we shall see in the following. Moreover, since $\Psi(0)$ is known ($= 0$) and $\Psi \in C^\infty$, it is possible to calculate the k-th derivative of Ψ at zero, for any k. This is a fundamental property that we shall exploit to calculate the bilinear and trilinear functions occurring in the computations of the normal forms [8].

From Eqs. (1), it is evident that (i) the equilibria of the system lie on the plane $x_1 = -x_2$, (ii) their positions depend on p_2 only, and (iii) the origin $E_0 = (0, 0, 0)$ is a trivial equilibrium point for any $\boldsymbol{p}$. The stabilities of the equilibria depend on both parameters p_1 and p_2, as it follows from the Jacobian matrix of the system (that can be written only partially in explicit form):

$$A = \begin{bmatrix} -1 & -1 & 0 \\ 2 + p_1 & 1 + p_1 & -p_2 \\ \frac{p_3 \sqrt{p_5^2+\Psi^2}}{1+\sqrt{p_5^2+\Psi^2}} & 0 & -p_3\left(\frac{p_3 \sqrt{p_5^2+\Psi^2}}{1+\sqrt{p_5^2+\Psi^2}} + p_4 \cosh(x_3)\right) \end{bmatrix} \tag{2}$$

It is easy to check that system (1) is invariant with respect to the transformation $T : \boldsymbol{x} \longrightarrow -\boldsymbol{x}$. In other terms, we can define a matrix $R = -I$ (with I identity matrix in $\mathbb{R}^3$) such that $R\,\boldsymbol{f}(\boldsymbol{x}; \boldsymbol{p}) = \boldsymbol{f}(R\,\boldsymbol{x}; \boldsymbol{p})$. According to [8], this means that system (1) is $\mathbb{Z}_2$-equivariant and that the set of points $X^+ = \{x \in \mathbb{R}^3 \mid R\,x = x\}$ reduces to the zero-dimensional set $X^+ = \{E_0 = (0, 0, 0)\}$, whereas its (three-dimensional) complementary set is $X^- = \mathbb{R}^3 \setminus \{E_0\}$. As a consequence, the equilibria and periodic solutions of the system can be either *fixed* (*i.e.*, invariant under the symmetry transformation T) or *symmetric* (*i.e.*, there are two twin solutions, each of which can be obtained by applying the transformation T to the other one). Henceforth, we shall denote as F-cycles and S-cycles the fixed and the symmetric limit cycles, respectively. The same holds, *mutatis mutandis*, for equilibria. Excepted for E_0, which is of F-type, all the system equilibria are necessarily of S-type. We point out that all the solutions admitted by a $\mathbb{Z}_2$-equivariant system can undergo a restricted set of codimension-1 bifurcations [8].

3. The equilibrium E_0

The (local) bifurcations concerning the equilibrium E_0 can be studied through normal forms theory. Henceforth, the Jacobian matrix (2) evaluated at E_0 will be denoted as J_0.

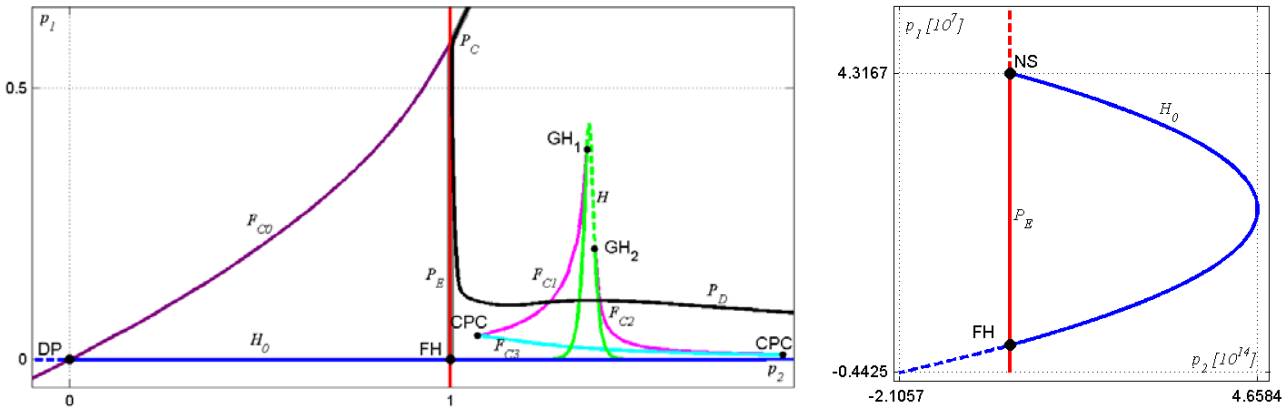

(*a*) (*b*)

Figure 1: Bifurcation curves (a). Complete overview (on a much larger scale) of the curves H_0 and P_E (b).

3.1. Pitchfork bifurcation

One of the eigenvalues of J_0 vanishes at the bifurcation value $p_2^{BP} = 1 + p_4\frac{1+p5}{p5}$. The eigenvector v associated with the vanishing eigenvalue is in X^-. Owing to the $\mathbb{Z}_2$ symmetry of the system, this is sufficient (see [8] for details) to show that the restriction of the system to the center manifold is topologically equivalent to a symmetric pitchfork bifurcation, resulting in the appearance of two symmetric equilibrium points, say E_+ and E_-.

The pitchfork bifurcation curve P_E on the plane (p_2, p_1) is represented in red in Fig. 1. The sign of the coefficient of the third-order term in the the polynomial restriction of the system to the center manifold determines the nature either supercritical (solid line in Fig. 1b) or subcritical (dashed line) of the pitchfork bifurcation. For the supercritical case, the following condition holds:

$$p_1 \leq \frac{1 + p_5}{p_3p_4 + p_3p_5 + p_3p_4p_5} \tag{3}$$

We point out that the curve P_E is partially overlapped with another bifurcation curve (the gray curve P_C), that will be introduced in Sec. 4.3.

3.2. Hopf bifurcation

The matrix J_0 has two imaginary eigenvalues at

$$\begin{cases} p_1 = \frac{-1+\omega^2}{b} \\ p_2 = \frac{(-1+\omega^2)(b^2+\omega^2)}{a\,b} \end{cases} \tag{4}$$

where a, b, and ω are quite complex combinations of the system parameters. In particular, ω is the angular frequency of the F-cycle (henceforth denoted as C_0) appearing around E_0 at the bifurcation point. Keeping in mind that ω must be positive, the Hopf bifurcation curve H_0 defined by Eq. (4) is the blue line in Fig. 1b (Fig. 1a shows just a detail around the origin of the parameter plane). Such a curve is parameterized by ω, which vanishes at the end point labelled by NS, where E_0 has two coincident eigenvalues at 0. For this reason, in this point the parametric curve Eq. (4) no longer denotes a Hopf bifurcation but simply a *neutral saddle* (NS) point. Another significant point (labelled by FH) is the other intersection between H_0 and P_E. At this *Fold-Hopf* bifurcation point, J_0 has one zero eigenvalue and a pair of purely imaginary eigenvalues.

On H_0, we can apply the projection technique [8], thus finding (i) a polynomial approximation topologically equivalent to the Hopf normal form and (ii) an analytical expression for the first Lyapunov coefficient. Such a coefficient turns out to change its sign with p_2, *i.e.*, the Hopf bifurcation is supercritical for $p_2 > 0$ and subcritical elsewhere (*cf.* Fig. 1(a)). Actually, for $p_2 = 0$ the linear part of the system does not depend on the nonlinear one, then E_0 degenerates to a *center* and the local state portrait of the system around E_0 is characterized by the presence of infinite non-isolated neutral cycles. This is the reason why the degenerate point $(p_2, p_1) = (0, 0)$ is labelled by DP. The presence of DP is due to an inadequacy of the model Eq. (1). An accurate study of the system dynamics near this point (through the singular perturbation theory) would be mathematically intriguing though not significant for our purposes, thus we limited ourselves to a numerical analysis, as we shall see in the next section.

4. Equilibrium points E_+ and E_-

In this section, we propose an analysis of the (local) bifurcations concerning the equilibria E_+ and E_- appearing at the right of the curve P_E. These equilibria cannot be studied analytically due to the implicit expression of the function Ψ, though they can be found and followed by varying the parameters through numerical continuation tools (and by numerically solving the implicit equation (1d) in system (1)). Both of them are stable in the parameter region at the right of P_E and below the curve H (see the green curve in Fig. 1a), which marks a Hopf bifurcation. Such a bifur-

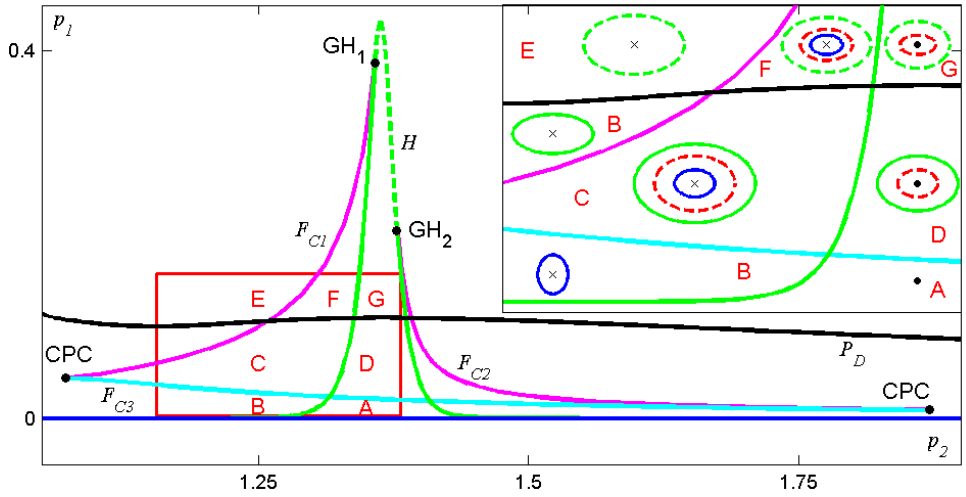

Figure 2: Bifurcation scenario around GH_1 and GH_2. The upper-right box is an enlargement of the red rectangle containing a qualitative sketch of the state portraits corresponding to the labelled regions. The blue cycle is C_{a+}, the red cycle is C_U, and the green cycle is C_{b+}.

cation can be either supercritical (solid line) or subcritical (dashed line), depending on the numerically calculated first Lyapunov coefficient, which changes its sign at the points GH_1 and GH_2 (see the enlargement of Fig. 1a in Fig. 2). The two F-cycles that appear around E_+ and E_- crossing H will be called C_{a+} and C_{a-}, respectively.

Henceforth, we shall refer to the invariant sets with index '+', knowing that the same considerations hold, *mutatis mutandis*, for the R-conjugate invariant set. Moreover, in the figures sketching state portraits, the symbol '×' denotes an unstable equilibrium, whereas the black dot indicates a stable equilibrium. For the cycles, the solid and dashed lines denote stability and instability, respectively.

4.1. System unfolding around GH_1 and GH_2

In Figs. 1a and 2, the magenta bifurcation curves labelled by F_{C1} and F_{C2} denote the fold bifurcation curves of cycles originating (according to the theory [8]) from the generalized Hopf points GH_1 and GH_2, respectively. The system unfolding around such codimension-2 points is well known, but in order to better understand the global bifurcation scenario, we shall describe the role played by the involved limit cycles on a larger scale, by making reference to Fig. 2. The two curves F_{C1} and F_{C2} turn out to be two branches of a single bifurcation curve, connected trough a third branch (the cyan curve F_{C3}) joining two cusp points (CPC) where three limit cycles (*i.e.*, the blue cycle C_{a+}, created through H, and the green and red cycles C_{b+} and C_U, respectively, created through F_{C3}) simultaneously collide and disappear. In Fig. 2, the region labels are reported only at the left of the abscissa of the maximum of the Hopf bifurcation curve H. At the right of such an abscissa the regions could be labelled in a symmetric way. The qualitative state portraits corresponding to the different regions are reported in the upper-right box of Fig. 2. Moving within region B clockwise around the left cusp point, the (stable) limit cycle C_{a+} smoothly changes into C_{b+}. The numerically-detected black bifurcation curve P_D in Fig. 2 marks a supercritical period doubling bifurcation for the cycle C_{b+}. The period-two stable cycle originating from such a bifurcation is not reported in Fig. 2 as it is not necessary to clarify, even on larger scale, the bifurcation scenario around the points GH_1 and GH_2. For the sake of completeness, we remark that P_D is the first bifurcation of a Feigenbaum route to chaos (see [5]).

4.2. System unfolding around DP

Figure 3 shows the system unfolding around the bifurcation point DP. We shall describe the unfolding moving counterclockwise around DP from region A. In region A, there is only the (stable) equilibrium point E_0, that undergoes a supercritical Hopf bifurcation (thus becoming unstable and generating the stable F-cycle C_0) when we cross the solid blue curve H_0^+ (region B). Among the infinite non-isolated cycles existing at DP, just two of them survive in region B, *i.e.*, the stable cycle C_0 and an unstable (numerically detected) F-cycle, say C_{0U}, that appears with very large amplitude on a line practically coincident with H_0^+. The two cycles C_0 and C_{0U} collide and disappear when we cross the purple curve F_{C0} (see also Fig. 1a). Thus, in region C there is only the (unstable) equilibrium point E_0. Such a point undergoes a subcritical Hopf bifurcation (thus becoming stable and generating the unstable cycle C_0) when we cross the dashed blue curve H_0^- (region D). Also in region D we have only two of the infinite non-isolated cycles existing in DP, *i.e.*, the unstable cycle C_0 and a stable F-cycle, say C_{0S}, that can be easily detected numerically; C_{0S} as well appears with very large amplitude

on a line practically coincident with H_0^-. The two cycles C_0 and C_{0S} collide and disappear when we cross the curve F_{C0}, thus coming back to region A.

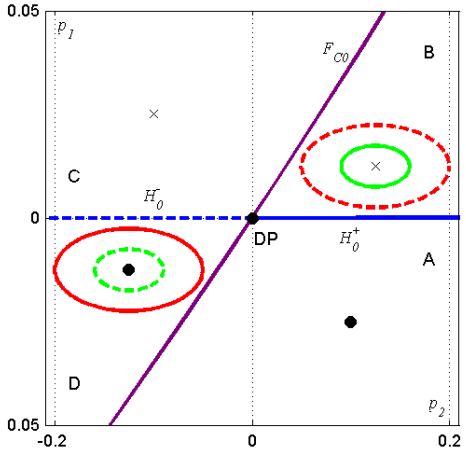

Figure 3: System unfolding around DP. The green cycle is C_0 and the red cycle is C_{0U}.

4.3. System unfolding around FH

Figure 4 shows the system unfolding around the *Fold-Hopf* bifurcation point FH. In region A, there is only the (stable) equilibrium point E_0, that undergoes a supercritical pitchfork bifurcation (thus becoming unstable and generating the stable equilibrium point E_+) when we cross the red curve P_E (region B). If we move counterclockwise around FH, when we cross the the solid blue curve H_0^+, E_0 undergoes a supercritical Hopf bifurcation on its two-dimensional stable manifold (thus generating the unstable cycle C_0). When we cross the green (supercritical) Hopf bifurcation curve H, E_+ becomes unstable and generates the stable cycle C_{a+}. Then, we cross two distinct curves (hardly distinguishable in Fig. 4), the supercritical pitchfork of cycles bifurcation curve P_C (involving C_{a+} and C_0) and the supercritical pitchfork bifurcation curve P_E (involving E_+ and E_0). The curve P_C is represented in grey and can be viewed also in Fig. 1, where it appears superimposed partially to P_E and partially to F_{C0}. Thus, in region E the system has the unstable equilibrium point E_0 and the stable S-cycle C_0. Finally, when we cross again the the solid blue curve H_0^+, thus coming back to region A, C_0 disappears and E_0 becomes stable, thus completing the unfolding.

5. Concluding remarks

In this paper we have presented a bifurcation analysis of a nonlinear oscillator based on hysteresis. The analysis, carried out by resorting to both continuation methods and theory of normal forms, concerns only local bifurcations of the equilibrium points and of some limit cycles strictly related to such equilibria. The system unfoldings around some significant points in the parameter plane have been proposed to better clarify the local bifurcation scenarios.

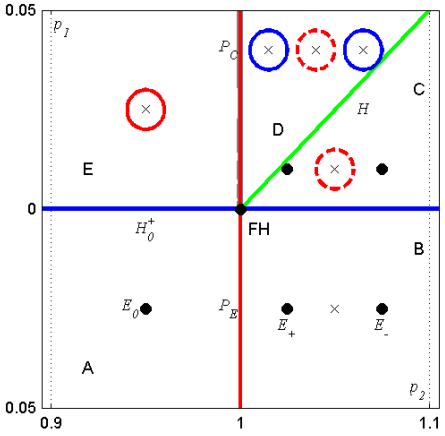

Figure 4: System unfolding around FH. The red cycle is C_0, and the blue cycles are C_{a+} and the other S-cycle C_{a-}.

Acknowledgments

Work supported by the MIUR, within the FIRB framework.

References

[1] M. Storace, M. Parodi, "Simple realisation of hysteresis chaos generator", *El. Lett.*, **34**, pp. 10–11, 1998.

[2] F. Bizzarri, M. Storace, L. Gardini, R. Lupini, "Bifurcation analysis of a PWL chaotic circuit based on hysteresis through a one-dimensional map", *Int. J. Bif. Chaos*, **11**, pp. 1911-1927, 2001.

[3] M. Storace, F. Bizzarri, "Basic bifurcation analysis of a hysteresis oscillator", *Int. J. CTA*, **29**, pp. 343-366, 2001.

[4] F. Bizzarri, M. Storace, "Two-dimensional bifurcation diagrams of a chaotic circuit based on hysteresis", *Int. J. Bif. Chaos*, **12**, pp. 43-69, 2002.

[5] F. Bizzarri, M. Storace, "Coexistence of attractors in an oscillator based on hysteresis", in *Proc. ISCAS'2002*, Scottsdale, Arizona, 26-29 May 2002, p. 1713.

[6] M. Bonnin, M. Gilli, P.P. Civalleri, "Analysis of a hysteretic oscillator through a mixed time-frequency domain approach", in *Proc. ISCAS'2005*, Kobe, Japan, 23-26 May 2005, in press.

[7] E. Doedel *et al.*, *AUTO 2000*, Comp. Sci. Dept., Concordia University, Montreal, Quebec, Canada, 2001.

[8] Y. Kuznetsov, *Elements of Applied Bifurcation Theory*, Springer-Verlag, New York, NY, 2nd ed., 1998.